Title Page

PNAS research report, direct submission

Classification: - Biological Sciences
- Microbiology

Suppression of co-stimulation by human cytomegalovirus promotes evasion of cellular immune defenses

Short Title: HCMV regulates CD58 to control T and NK cells

Eddie C.Y. Wang[1*], Mariana Pjechova[1,2*], Katie Nightingale[3], Virginia-Maria Vlahava[1], Mihil Patel[1], Eva Ruckova[1,2], Simone Forbes[1], Luis Nobre[3], Robin Antrobus[3], Dawn Roberts[1], Ceri A. Fielding[1], Sepehr Seirafian[1], James Davies[1], Isa Murrell[1], Betty Lau[4], Gavin S. Wilkie[4], Nicolás M. Suárez[4], Richard J. Stanton[1], Borivoj Vojtesek[2], Andrew Davison[4], Paul J. Lehner[3], Michael P. Weekes[3*], Gavin W.G. Wilkinson[1*], Peter Tomasec[†1*]

[1]Cardiff University School of Medicine, Division of Infection and Immunity, Henry Wellcome Building, Heath Park, Cardiff CF14 4XN, UK
[2]Regional Centre for Applied Molecular Oncology (RECAMO), Masaryk Memorial Cancer Institute, Zluty Kopec 7, 65653 Brno, Czech Republic
[3]Cambridge Institute for Medical Research, University of Cambridge, Hills Road, Cambridge CB2 0XY, UK
[4] MRC-University of Glasgow Centre for Virus Research, Sir Michael Stoker Building, 464 Bearsden Road, Glasgow G61 1QH, UK

*these authors contributed equally to this study

Corresponding Author:
Eddie C. Y. Wang, Cardiff University School of Medicine, Division of Infection and Immunity, Henry Wellcome Building 1F-07, Heath Park, Cardiff CF14 4XN, UK; +44-2920687035; WangEC@cf.ac.uk

[†] deceased

Keywords:
HCMV, immune modulation, CTL, T-cell, NK cell, CD58, LFA3, CD2, UL148, UL/b'

Abstract

CD58 is an adhesion molecule that is known to play a critical role in co-stimulation of effector cells and is intrinsic to immune synapse structure. Herein, we describe the first virally-encoded gene that inhibits CD58 surface expression. Human cytomegalovirus (HCMV) UL148 was necessary and sufficient to promote intracellular retention of CD58 during HCMV infection. Blocking studies with antagonistic anti-CD58 mAb and an HCMV UL148 deletion mutant (HCMVΔUL148) with restored CD58 expression demonstrated that the CD2/CD58 axis was essential for the recognition of HCMV-infected targets by $CD8^+$ HCMV-specific cytotoxic T lymphocytes (CTLs). Further, challenge of peripheral blood mononuclear cells *ex vivo* with HCMVΔUL148 increased both CTL and natural killer (NK) cell degranulation against HCMV-infected cells, including NK-driven antibody-dependent cellular cytotoxicity, showing that UL148 is a modulator of the function of multiple effector cell subsets. Our data stress the impact of HCMV immune evasion functions on shaping the immune response, highlighting the capacity for their potential use in modulating immunity during the development of anti-HCMV vaccines and HCMV-based vaccine vectors.

Significance statement

HCMV is the major infectious cause of developmental disorders in babies due to its capacity to cross the placenta. HCMV is also a major pathogen in transplant recipients and HIV-AIDS patients. Despite inducing the strongest immune responses observed for any human pathogen, HCMV evades host defenses and persists for life. We report a novel viral stealth strategy. HCMV UL148 reduces surface expression of a key cell adhesion molecule (CD58), impairing the ability of NK and T cells to be activated by HCMV-infected cells. This is the first description of a viral gene targeting this pathway. Our findings highlight a role for CD58 in recognition of HCMV-infected cells and may be relevant for development of future antiviral therapies.

\body

Introduction

Human cytomegalovirus (HCMV; species *Human betaherpesvirus 5*), is the major viral cause of congenital birth defects and an important pathogen capable of causing severe disease in immunocompromised and immune-naïve individuals. HCMV is noted for inducing the most potent cellular immune responses observed for any human pathogen. These responses, including expansions of cytotoxic T-lymphocytes (CTLs) and natural killer (NK) cells of a specific phenotype, are large and are maintained for life (reviewed in (1, 2)). HCMV, however, is not cleared by the host following primary infection. The mechanisms that underpin the ability of the virus to endure in the presence of such immunity has been the target of intense study, with the hope that the knowledge gained will inform the generation of anti-HCMV vaccines and also vaccine design, for which the maintenance of induced immune responses is paramount. Indeed, HCMV is being pursued as a vaccine vector in its own right as redirection of anti-CMV immunity can clear pathogens otherwise capable of persisting in their host (3, 4). The study of HCMV-encoded genes and proteins has revealed many strategies designed to avoid innate and adaptive immunity, which have defined a number of basic immune pathways essential to CTL and NK activity. These include at least four functions that inhibit HLA-I expression and ten that impair NK cell activation (reviewed in (5, 6)).

CTLs and NK cells use the supramolecular adhesion complex (SMAC) at the immune synapse (IS) to interact with their targets. The SMAC is a tightly packed intercellular complex of adhesion molecules and receptor/ligand pairs where antigen presentation and signaling take place, which regulate the secretion of cytotoxic granules and cytokines from the effector cells (7-9). There are many descriptions of HCMV acting to prevent expression of activating ligands and promote the expression of inhibitory receptors on the target cell surface, but reports of immune evasion mechanisms able to impede formation of IS structure have been limited to remodeling of the target cell actin cytoskeleton (10).

CD58 (LFA-3) on target cells acts to promote cell-to-cell adhesion and IS formation, and to provide a co-stimulatory signal through its receptor, CD2, on effectors (11-23). Recent studies have highlighted the importance of CD2 engagement for co-stimulation of $CD4^+$ T-cells in HCMV infection (24) and adaptive NK cells (25, 26), and have identified the CD2/CD58 axis as the primary co-stimulatory pathway for $CD28^-CD8^+$ CTLs (19, 27, 28). Cell surface expression of CD58 has been reported to be either upregulated (29, 30) or downregulated (31) by HCMV infection depending on the HCMV strain used. The aim of

our study was to dissect this phenomenon, thereby determining the functional relevance of regulating CD58 expression on HCMV-infected cells. We describe the identification of the first viral-encoded gene responsible for downregulating CD58 and detail the broad impact of this novel function on both CTL and NK cell recognition in the context of HCMV infection.

Results

HCMV UL148 is a novel viral function down-regulating cell surface expression of CD58

HCMV strain AD169 has previously been reported to upregulate CD58 (29, 30), whereas proteomic analysis with low passage HCMV strain Merlin has suggested the opposite (31). We confirmed these effects directly by flow cytometry (Fig.1). AD169 has suffered a spontaneous deletion in its genome during *in vitro* culture, involving a 15kb sequence designated the U_L/*b*' region (32). We therefore investigated whether the function responsible for CD58 downregulation resided within U_L/*b*'. Surface expression of CD58 was analyzed in cells infected with a complete library of HCMV strain Merlin U_L/*b*' single gene deletion mutants (loss of function screen, Fig .2A) and an adenovirus vector library over-expressing each U_L/*b*' gene individually (gain of function screen, Fig.2B, Fig.S1). Both screens identified HCMV UL148 as the gene responsible, with loss of UL148 from HCMV strain Merlin (referred to as HCMV∆UL148) (Fig.S2) resulting in CD58 upregulation (Fig.2A, C), and ectopic expression of UL148 resulting in CD58 downregulation (Fig.2B, D).

To screen for additional cell surface targets of UL148, we used plasma membrane profiling (PMP) of cells infected with HCMV, comparing Merlin to HCMV∆UL148. Filtering for proteins with Ig-, MHC, Cadherin, C-type lectin and TNF InterPro functional domains (31, 33) was used to extend interrogation of UL148, focusing the analysis on immune receptors and ligands directly involved in NK or CTL functions (Fig.2E, Dataset S1 'Summary'). This proteomic analysis identified CD58 as the only cell surface molecule targeted by UL148 that fell within these categories (Fig.2E).

CD58 is retained within the cell by UL148

Expression of CD58 was then studied during the course of HCMV infection. CD58 was gradually downregulated from the cell surface (Fig.1), whereas expression increased in whole cell lysates (Fig.3A). A faster migrating EndoH-sensitive CD58 glycoform accumulated in HCMV-infected cells and contrasted with the EndoH-resistant form detected in cells infected with HCMV∆UL148 (Fig.3A & B). This result is consistent with UL148 retaining CD58 as an immature precursor in the ER prior to processing through the Golgi complex. This model was further supported by co-immunoprecipitation of CD58 with UL148 from infected cells visualized either using immunoprecipitation with V5-tagged UL148 and Western blotting with anti-CD58 (Fig.3C) or in a global proteomic analysis

using stable isotope labeling by amino acids in cell culture and immunoprecipitation (SILAC-IP) (Fig.S3). In conclusion, UL148 was both necessary and sufficient to mediate cell surface down-regulation and intracellular retention of CD58.

UL148 is a potent modulator of CTL function

The functional impact of CD58 regulation on CTL recognition was investigated in the context of HCMV infection by using HLA-A2-restricted $CD8^+$ CTL lines generated to HCMV-IE1 VLEETSMVL (VLE) and HCMV-pp65 NLVPMVATV (NLV) peptides. These lines were tested by using CD107a degranulation assays and intracellular cytokine staining to detect cytokine production against autologous fibroblasts (uninfected or infected with Merlin or HCMVΔUL148) pulsed with a range of peptide concentrations. Absence of peptide led to minimal CTL activation. Peptide pulsing of uninfected cells resulted in a large increase in degranulation, which was significantly impaired by infection with HCMV strain Merlin. Deletion of UL148 resulted in recovery of degranulation in both CTL lines against HCMV-infected fibroblasts, including some experiments in which activation by HCMVΔUL148 was equivalent to that observed by peptide-pulsed uninfected cells (Fig.4A). A similar effect was observed for cytokine production in a third CTL line (Fig.S4). This occurred even though both Merlin and HCMVΔUL148 down-regulated HLA class-I evenly by more than tenfold (Fig.4B), indicating that these effects were independent of signals supplied through TCR recognition of HLA-I at that peptide dose. UL148 function could therefore compensate for more than tenfold differences in HLA-I expression. Significant differences in degranulation between Merlin and HCMVΔUL148 were observed over a narrow peptide range, with close to a doubling of the proportion of activated $CD8^+$ CTLs occurring at 1μg/ml peptide, corresponding to a molar concentration of ~1μM. Doubling or decreasing the peptide dose by 20-fold overcame these differences (Fig.4C).

CD58 co-stimulatory function occurs only in HCMV-infected cells

The specificity of the UL148 effect on CD58 was explored by using a monoclonal antibody (mAb) that inhibited CD2/CD58 interaction. Application of anti-CD58 mAb resulted in significant blocking of CTL activity towards cells infected with HCMVΔUL148 over a range of peptide concentrations, in some cases reducing it to the levels observed when using Merlin-infected cells as targets (Fig.4D). We performed a more detailed analysis that combined all blocking experiments by normalizing data to the isotype control in each experiment. These combined data showed that blocking of CD58 produced an effect that was observable even against Merlin-infected targets, that became significantly different from the blocking of activation by HCMVΔUL148 at the peak peptide concentration

(1µg/ml) (Fig.4E). Irrespective of higher levels of surface CD58 compared to HCMV-infected targets, CTL activation measured by CD107 degranulation against uninfected cells could not be reduced by anti-CD58 mAb treatment, regardless of the peptide concentration used (Fig.4E,F). This differential effect of peptide loading and targets implies that HCMV-specific $CD8^+$ CTLs are exquisitely sensitive to the context in which they receive activation signals, in that CD58-mediated co-stimulation became relevant only when these CTL were faced with an HCMV-infected target.

UL148 significantly alters the *ex vivo* PBMC response to HCMV-infected cells

The above data were generated using *in vitro* expanded T-cell lines. To test function in a more physiologically relevant setting, we challenged peripheral blood mononuclear cells (PBMC) *ex vivo* with fibroblasts infected with either Merlin or HCMV∆UL148 in the absence of exogenous peptide, comparing the degranulation responses of key effector cell subsets to the two viruses. In autologous assays and in the absence of peptide, $CD3^+CD8^+$ T-cells significantly increased their activation in response to HCMV∆UL148 in 3 of 9 subjects (Fig.4G). The CD2/CD58 axis has also been reported to be important in the activation of 'adaptive' NK cells defined through expression of CD57 and NKG2C, the expansion of which is associated with previous HCMV infection (25, 26). Responses of *ex vivo* NK cells were tested in the presence of Cytotect (purified IgG from HCMV-seropositive subjects) or IgG from HCMV-seronegative individuals, included as a negative control to measure antibody-dependent cellular cytotoxicity (ADCC) as well as standard NK cell function. NK cell function was measured against both allogeneic human fetal foreskin fibroblasts (HFFFs) and autologous HCMV-infected skin fibroblasts. The greatest effect of removing UL148 was observed in an allogeneic ADCC setting with smaller, but significant increases in NK cell activation in the absence of Cytotect (Fig.5A,B, Fig.S4). In an autologous setting, removing UL148 significantly increased the recognition of HCMV-infected targets only in the presence of Cytotect (Fig.5C). Further analysis to phenotype the responsive subset indicated it resided in $CD57^+$ NK cells (Fig.5D), with different subjects showing significantly different responses to ∆UL148 in one, other or both of $CD57^+NKG2C^-$ and $CD57^+NKG2C^+$ NK populations (Fig.5E). $CD57^-NKG2C^+$ populations were not analyzed because they represented less than 3% of total $CD3^-CD56^+$ NK cells in all but one subject.

Discussion

HCMV has become a paradigm for viral immune evasion, with the study of the activities of its genes and proteins unveiling many aspects of immune function. We have now identified HCMV UL148 as the first recognized virally encoded downregulator of the cell adhesion molecule CD58, the intracellular retention of which reduces *ex vivo* activation of both CTLs and NK cells. This function is compatible with UL148 being an ER-resident type 1 transmembrane glycoprotein containing an ER retention motif (RRR, at residues 314-316) (34, 35). The CD58/CD2 axis may become particularly important when infected target cells exhibit sub-optimal activation signals, for example due to the action of multiple HCMV-encoded immune evasins.

To date, UL148 has only been assigned one other viral function. In the HCMV strain TB40/E, UL148 disruption alters the ratio of glycoprotein H/glycoprotein L (gH/gL) complexes involved in virus entry, resulting in increased infectivity of epithelial cells, in part due to a direct interaction between UL148 and those complexes, and most likely in the ER (34). Our SILAC-IP analysis of proteins binding UL148 during infection with HCMV strain Merlin did not demonstrate a specific interaction with gH or gL (Fig.S3), suggesting underlying complexity in UL148 interactions associated with the HCMV strains used and their cellular tropisms. In this regard, there is also the possibility that the host proteins targeted by UL148 may differ depending on the cell type infected by HCMV, with our data derived from fibroblasts. The rhesus cytomegalovirus (RhCMV)-encoded ortholog of UL148 (Rh159) also has effects on virus tropism, although in this case disruption of the gene renders the virus unable to spread in epithelial cells (36). Further Rh159 exhibits immune regulatory functions, impairing the surface expression of the NKG2D ligands, MICA, MICB, ULBP1 and ULBP2 (37). Interestingly, although both Rh159 and UL148 act by binding to, and retaining intracellularly their target proteins, we and others have shown that UL148 does not bind any NKG2D ligands (37). In HCMV, these ligands are targeted by UL16, UL142, US9, US18 and US20 (5, 38). It will be interesting to determine whether there is a common theme of CMV-encoded ER-resident proteins that impact on both immune evasion and cell tropism.

It is intriguing that blocking the CD2/CD58 interaction with an anti-CD58 monoclonal antibody did not inhibit effector activation by uninfected peptide-pulsed target cells, but did inhibit activation by HCMV-infected cells (Fig. 4D-F). A degree of inhibition of Merlin-infected targets was expected since CD58 was still present albeit at a reduced level

compared to HCMVΔUL148-infected cells (Fig.4B). The absence of any effect against uninfected targets (which had equivalent levels of CD58 to HCMVΔUL148-infected cells) is surprising. The multiple immune evasion mechanisms employed by HCMV, such as impairment of TCR signaling via HLA-I downregulation or via inhibitory receptors such as LIR-1 binding HCMV UL18 (39), alter the balance of activating and inhibitory signals received by effectors. Our data are consistent with the concept that there is much more complexity in the way $CD8^+$ CTLs are activated by virally infected targets. HCMV-specific CTLs may be 're-tuned' to activate when exposed to infected targets in response to virus-encoded modulation of multiple activating and inhibitory ligands.

Some speculative evidence for this idea may be gleaned from the phenotype of HCMV-specific CTLs *in vivo*. HCMV drives massive, stable $CD8^+$ CTL expansions, but it is interesting to note that the detailed phenotype and responsiveness of these cells is unusual compared to those described in classical models of T-cell differentiation (reviewed recently in (1)). For example, continuous *in vitro* stimulation by anti-CD3/anti-CD28 beads induces hallmarks of exhaustion in $CD8^+$ T-cells ($IL\text{-}7R^{lo}$; and high levels of the immune cell inhibitor, programmed cell death protein 1 (PD1) (40)) that are reduced by co-stimulation through anti-CD2 signals (28). In contrast, although HCMV-specific $CD8^+$ CTLs have been reported as showing an exhausted/senescent and/or terminally differentiated phenotype, they exhibit proliferative capacity, the ability to change co-stimulatory and chemokine receptor-phenotype (41, 42) and do not show all the functionally associated classical markers of exhaustion such as PD1. They are generally $PD1^{lo}$ (39), whereas HCMV increases PD-L1 expression on infected cells (31), which would be consistent with HCMV-specific CTLs adapting to receive fewer inhibitory signals through the PD1/PD-L1 axis.

It is possible that immune adaptation occurs in all effector cells facing HCMV-infected targets, and that this leads to the unusual effector phenotypes observed in HCMV-seropositive subjects. With regard to NK cells, an 'adaptive' NK subset that is $CD57^+NKG2C^+FceR1^-$ is expanded in HCMV-infected individuals and involved in ADCC (43, 44). *In vitro* expanded $NKG2C^+$ NK cells exhibit higher levels of CD2 expression (45), which could aid activation in the face of lower levels of CD58 on target cells. We found that $CD57^+$ NK cells exhibited enhanced ADCC in response to targets infected with HCMVΔUL148 compared to Merlin, with different subjects showing an impact on either or both $NKG2C^-$ and $NKG2C^+$ NK cells within the $CD57^+$ population (Fig.5). This is not unexpected, as NKG2C null individuals show $CD57^+$ NK expansions following HCMV

infection (2), which exhibit a requirement for CD2 co-stimulation in their responses (26). The data are consistent with expanded effector subsets in HCMV-seropositive individuals showing greater responsiveness to an activation pathway being inhibited by HCMV.

Beyond CTL and NK cell recognition, it is notable that HCMV infection specifically induces cell surface expression of intercellular adhesion molecule 1 (ICAM1), which is reported to have an involvement equivalent to that of CD58 in formation of the SMAC (31, 46, 47). In the context of differential expression of such adhesion molecules. It is also tempting to speculate that ICAM1 may play an essential separate function in HCMV biology, and the specific downregulation of CD58 might provide an elegant mechanism for compensating for ICAM1 induction on infected cells. Indeed, ICAM1 is important in facilitating endothelial transmigration and permeability, and its induction could enhance dissemination of virus through host tissues (48) or play a role in direct cell-to-cell transfer of virus (49).

Finally, our data highlights that significant *ex vivo* ADCC does occur against HCMV-infected cells, even with HCMV strain Merlin, which encodes many NK cell immune evasion mechanisms and multiple Fc binding proteins (50). The impact of deleting UL148 on ADCC and general immune responses suggest that HCMV might be manipulated to drive the activation of multiple different effector cell types, making the emerging field of HCMV-based vector design all the more important for vaccine development.

Materials and Methods

Cells

Human fetal foreskin fibroblasts immortalized with human telomerase (HF-TERT), HF-TERTs transfected with the coxsackie-adenovirus receptor (HF-CAR), and TERT-immortalized donor dermal fibroblasts have been described previously (10). Cells were maintained in DMEM/10% fetal calf serum at 37°C/5% CO_2.

Viruses

HCMV strain Merlin RCMV1111/KM192298 ($RL13^-$, $UL128^-$) (51), AD169 varUK/BK000394, and Merlin recombinants containing single gene deletions in U_L/b' were generated as described previously (51) (SI1). Tagged HCMV recombinants were generated as described previously (38, 52) (SI1). Recombinant adenovirus vectors expressing individual HCMV UL/b' genes were generated as described previously (53) and validated for expression (54).

Antibodies and other reagents

All reagentss were obtained from Biolegend, except Aqua live/dead dye (ThermoFisher), CD3-PE-Cy7 (clone UCHT-1, Beckman Coulter), CD8-APC-H7 (clone SK1, BD Biosciences), CD56-PE (clone N901, Beckman Coulter), CD58 (Abcam) CD107a-FITC (clone H4A3, BD Biosciences), MHC class-I (clone W6/32, Serotec) NKG2C-PE (clone 134591, R&D systems), CD155 (5D1, (55)), actin (Sigma), V5-agarose (Abcam), V5 (Serotec), anti-mouse-AF647 (ThermoFisher), anti-mouse-HRP (BioRad), anti-rabbit-HRP (BioRad), mouse IgG, UL141 (56), EndoH (NEB), PNGaseF (NEB). Other reagents were CD8-APC (clone HIT8a), CD56-BV605 (clone HCD56), CD57-APC (clone HNK-1), CD58 (clone TS2/9), CD107a-PerCP-Cy5.5 (clone H4A3), TNFα-BV421 (clone Mab11), IFNγ-PE-Cy7 (4S.B3), MHC class-I-PE (clone W6/32).

Flow cytometry

For HCMV infections, adherent cells were harvested with TripLE Express (Thermofisher) or HyQTase™ (GE Healthcare), stained in PBS/1%BSA buffer at 4°C with relevant antibodies, fixed with 4% paraformaldehyde and analyzed on an Accuri C6 flow cytometer (BD Biosciences) and with Accuri C6 software. For CD107a degranulation assays, data were gathered on an 11-color Attune NxT flow cytometer (ThermoFisher) and analyzed using Attune NxT or FlowJo V10 software.

Immunoblotting

Cells were lysed and boiled in reducing denaturing Nu-PAGE lysis buffer, and protein samples were separated on Nu-PAGE gels, transferred onto nitrocellulose membrane (GE Life Sciences), stained with relevant antibodies and Supersignal West Pico chemiluminescent substrate and imaged on Hyperfilm-MP (GE Life Sciences). In co-immunoprecipitation experiments, cells were lysed in Triton X-100 lysis buffer, and protein complexes were captured with V5-agarose prior to SDS-PAGE and immunoblotting.

NK and T-cell assays

HCMV-specific CTL lines were grown from PBMCs stimulated with irradiated (6000 RADs) autologous, peptide-coated fibroblasts as described previously (10). Degranulation assays were performed as described previously (57), using effector:target ratios of 10:1. The targets were pulsed with peptide at various concentrations and the excess washed off, while for blocking studies, a final concentration of 10 µg/ml anti-CD58 mAb, TS2/9, was used. Statistical testing of data was carried out by using Graphpad Prism 5.0 for ANOVAs with Tukey's multiple comparisons post-tests; $p<0.05$ was considered significant. Assays detecting *ex vivo* PBMC responses were carried out as described previously (58), with adaptation to a CD107a degranulation readout as described (57) and using multicolor flow cytometry to identify responding $CD3^+CD8^+$ T-cells, $CD3^-CD56^+$ NK cells and populations defined by expression of CD57 and NKG2C. Cytotect (Biotest) or IgG purified from HCMV-seronegative subjects was incubated with targets for 10 mins at 37˚C at a concentration of 100 µg/ml prior to addition of an equivalent volume of effectors.

Proteomics

Proteomics was performed as described previously (31). Briefly, plasma membrane glycoproteins were oxidized with sodium metaperiodate and then biotinylated with aminoxybiotin (Cambridge Bioscience) prior to lysis of cells with Triton X-100. Biotinylated glycoproteins were captured with streptavidin agarose, and then washed, denatured, alkylated and digested on beads with Trypsin (Gibco). Peptides were fractionated by using strong cation exchange. Enriched peptides were labeled with tandem mass tag (TMT) reagents, combined at a 1:1 ratio, and then pre-fractionated by offline high-pH-reversed-phase chromatography (Agilent). Mass spectrometry and data analysis were performed as described previously by using an Orbitrap Fusion. P-values were estimated using Benjamini-Hochberg-corrected significance A or Significance B values from Perseus version 1.2.0.16 (59). SILAC-IP experiments were conducted and analyzed as described previously (10).

Ethics statement

Healthy adult volunteers provided blood and dermal fibroblasts for this study after providing written informed consent. The study was approved by the Cardiff University School of Medicine Research Ethics Committee ref. nos: 10/20 and 16/52.

Acknowledgements

The study was supported by MRC and Wellcome Trust grants G1000236, MR/P001602/1, WT090323MA, MR/L008734/1 (ECYW, VV, SF, DR, CAF, SS, IM, MiP, RJS, GWW, PT), MC_UU_12014/3 (GSW, NMS, BL, AD), MEYS – NPS I – LO1413 (MP, ER), Czech Science Foundation project no. P206/12/G151 (BV), Wellcome Trust Senior Clinical Research Fellowship 108070 (MPW), and Wellcome Trust Principal Research Fellowship 101835 (PJL).

References

1. Klenerman P & Oxenius A (2016) T cell responses to cytomegalovirus. *Nat Rev Immunol* 16(6):367-377.
2. Goodier MR, *et al.* (2014) Rapid NK cell differentiation in a population with near-universal human cytomegalovirus infection is attenuated by NKG2C deletions. *Blood* 124(14):2213-2222.
3. Hansen SG, *et al.* (2013) Cytomegalovirus vectors violate CD8+ T cell epitope recognition paradigms. *Science* 340(6135):1237874.
4. Hansen SG, *et al.* (2013) Immune clearance of highly pathogenic SIV infection. *Nature* 502(7469):100-104.
5. Wilkinson GW, *et al.* (2008) Modulation of natural killer cells by human cytomegalovirus. *J Clin Virol* 41(3):206-212.
6. Halenius A, Gerke C, & Hengel H (2015) Classical and non-classical MHC I molecule manipulation by human cytomegalovirus: so many targets-but how many arrows in the quiver? *Cell Mol Immunol* 12(2):139-153.
7. Davis DM, *et al.* (1999) The human natural killer cell immune synapse. *Proc Natl Acad Sci U S A* 96(26):15062-15067.
8. Grakoui A, *et al.* (1999) The immunological synapse: a molecular machine controlling T cell activation. *Science* 285(5425):221-227.
9. Monks CR, Freiberg BA, Kupfer H, Sciaky N, & Kupfer A (1998) Three-dimensional segregation of supramolecular activation clusters in T cells. *Nature* 395(6697):82-86.
10. Stanton RJ, *et al.* (2014) HCMV pUL135 remodels the actin cytoskeleton to impair immune recognition of infected cells. *Cell Host Microbe* 16(2):201-214.
11. Beyers AD, Spruyt LL, & Williams AF (1992) Molecular associations between the T-lymphocyte antigen receptor complex and the surface antigens CD2, CD4, or CD8 and CD5. *Proc Natl Acad Sci U S A* 89(7):2945-2949.
12. Bierer BE & Hahn WC (1993) T cell adhesion, avidity regulation and signaling: a molecular analysis of CD2. *Semin Immunol* 5(4):249-261.
13. Brown MH, Cantrell DA, Brattsand G, Crumpton MJ, & Gullberg M (1989) The CD2 antigen associates with the T-cell antigen receptor CD3 antigen complex on the surface of human T lymphocytes. *Nature* 339(6225):551-553.
14. Davis SJ, Ikemizu S, Wild MK, & van der Merwe PA (1998) CD2 and the nature of protein interactions mediating cell-cell recognition. *Immunol Rev* 163:217-236.
15. Dustin ML, Selvaraj P, Mattaliano RJ, & Springer TA (1987) Anchoring mechanisms for LFA-3 cell adhesion glycoprotein at membrane surface. *Nature* 329(6142):846-848.
16. Gassmann M, Amrein KE, Flint NA, Schraven B, & Burn P (1994) Identification of a signaling complex involving CD2, zeta chain and p59fyn in T lymphocytes. *Eur J Immunol* 24(1):139-144.
17. Holter W, Schwarz M, Cerwenka A, & Knapp W (1996) The role of CD2 as a regulator of human T-cell cytokine production. *Immunol Rev* 153:107-122.
18. Kaizuka Y, Douglass AD, Vardhana S, Dustin ML, & Vale RD (2009) The coreceptor CD2 uses plasma membrane microdomains to transduce signals in T cells. *J Cell Biol* 185(3):521-534.
19. Leitner J, Herndler-Brandstetter D, Zlabinger GJ, Grubeck-Loebenstein B, & Steinberger P (2015) CD58/CD2 Is the Primary Costimulatory Pathway in Human CD28-CD8+ T Cells. *J Immunol* 195(2):477-487.
20. Meuer SC, *et al.* (1984) An alternative pathway of T-cell activation: a functional role for the 50 kd T11 sheep erythrocyte receptor protein. *Cell* 36(4):897-906.
21. Selvaraj P, *et al.* (1987) The T lymphocyte glycoprotein CD2 binds the cell surface ligand LFA-3. *Nature* 326(6111):400-403.

22. Siliciano RF, Pratt JC, Schmidt RE, Ritz J, & Reinherz EL (1985) Activation of cytolytic T lymphocyte and natural killer cell function through the T11 sheep erythrocyte binding protein. *Nature* 317(6036):428-430.
23. Yang JJ, Ye Y, Carroll A, Yang W, & Lee HW (2001) Structural biology of the cell adhesion protein CD2: alternatively folded states and structure-function relation. *Curr Protein Pept Sci* 2(1):1-17.
24. Shiao SL, *et al.* (2007) Human effector memory CD4+ T cells directly recognize allogeneic endothelial cells in vitro and in vivo. *J Immunol* 179(7):4397-4404.
25. Rolle A, *et al.* (2016) CD2-CD58 interactions are pivotal for the activation and function of adaptive natural killer cells in human cytomegalovirus infection. *Eur J Immunol* 46(10):2420-2425.
26. Liu LL, *et al.* (2016) Critical Role of CD2 Co-stimulation in Adaptive Natural Killer Cell Responses Revealed in NKG2C-Deficient Humans. *Cell Rep* 15(5):1088-1099.
27. Bruns T, *et al.* (2015) CMV infection of human sinusoidal endothelium regulates hepatic T cell recruitment and activation. *J Hepatol* 63(1):38-49.
28. McKinney EF, Lee JC, Jayne DR, Lyons PA, & Smith KG (2015) T-cell exhaustion, co-stimulation and clinical outcome in autoimmunity and infection. *Nature* 523(7562):612-616.
29. Grundy JE & Downes KL (1993) Up-regulation of LFA-3 and ICAM-1 on the surface of fibroblasts infected with cytomegalovirus. *Immunology* 78(3):405-412.
30. Fletcher JM, Prentice HG, & Grundy JE (1998) Natural killer cell lysis of cytomegalovirus (CMV)-infected cells correlates with virally induced changes in cell surface lymphocyte function-associated antigen-3 (LFA-3) expression and not with the CMV-induced down-regulation of cell surface class I HLA. *J Immunol* 161(5):2365-2374.
31. Weekes MP, *et al.* (2014) Quantitative temporal viromics: an approach to investigate host-pathogen interaction. *Cell* 157(6):1460-1472.
32. Cha TA, *et al.* (1996) Human cytomegalovirus clinical isolates carry at least 19 genes not found in laboratory strains. *J Virol* 70(1):78-83.
33. Vivier E, Tomasello E, Baratin M, Walzer T, & Ugolini S (2008) Functions of natural killer cells. *Nat Immunol* 9(5):503-510.
34. Li G, Nguyen CC, Ryckman BJ, Britt WJ, & Kamil JP (2015) A viral regulator of glycoprotein complexes contributes to human cytomegalovirus cell tropism. *Proc Natl Acad Sci U S A* 112(14):4471-4476.
35. ELM (2015) The Eukaryotic Linear Motif resource for functional sites in proteins.
36. Lilja AE, Chang WL, Barry PA, Becerra SP, & Shenk TE (2008) Functional genetic analysis of rhesus cytomegalovirus: Rh01 is an epithelial cell tropism factor. *J Virol* 82(5):2170-2181.
37. Sturgill ER, *et al.* (2016) Natural Killer Cell Evasion Is Essential for Infection by Rhesus Cytomegalovirus. *PLoS Pathog* 12(8):e1005868.
38. Fielding CA, *et al.* (2014) Two novel human cytomegalovirus NK cell evasion functions target MICA for lysosomal degradation. *PLoS Pathog* 10(5):e1004058.
39. Hertoghs KM, *et al.* (2010) Molecular profiling of cytomegalovirus-induced human CD8+ T cell differentiation. *J Clin Invest* 120(11):4077-4090.
40. Francisco LM, Sage PT, & Sharpe AH (2010) The PD-1 pathway in tolerance and autoimmunity. *Immunol Rev* 236:219-242.
41. Gandhi MK, *et al.* (2003) Late diversification in the clonal composition of human cytomegalovirus-specific CD8+ T cells following allogeneic hemopoietic stem cell transplantation. *Blood* 102(9):3427-3438.
42. Waller EC, *et al.* (2007) Differential costimulation through CD137 (4-1BB) restores proliferation of human virus-specific "effector memory" (CD28(-) CD45RA(HI)) CD8(+) T cells. *Blood* 110(13):4360-4366.

43. Guma M, *et al.* (2004) Imprint of human cytomegalovirus infection on the NK cell receptor repertoire. *Blood* 104(12):3664-3671.
44. Guma M, *et al.* (2006) Expansion of CD94/NKG2C+ NK cells in response to human cytomegalovirus-infected fibroblasts. *Blood* 107(9):3624-3631.
45. Beziat V, *et al.* (2013) NK cell responses to cytomegalovirus infection lead to stable imprints in the human KIR repertoire and involve activating KIRs. *Blood* 121(14):2678-2688.
46. Kronschnabl M & Stamminger T (2003) Synergistic induction of intercellular adhesion molecule-1 by the human cytomegalovirus transactivators IE2p86 and pp71 is mediated via an Sp1-binding site. *J Gen Virol* 84(Pt 1):61-73.
47. Huppa JB & Davis MM (2003) T-cell-antigen recognition and the immunological synapse. *Nat Rev Immunol* 3(12):973-983.
48. Bentz GL, *et al.* (2006) Human cytomegalovirus (HCMV) infection of endothelial cells promotes naive monocyte extravasation and transfer of productive virus to enhance hematogenous dissemination of HCMV. *J Virol* 80(23):11539-11555.
49. Murrell I, *et al.* (2017) The pentameric complex drives immunologically covert cell-cell transmission of wild-type human cytomegalovirus. *Proc Natl Acad Sci U S A* 114(23):6104-6109.
50. Corrales-Aguilar E, *et al.* (2014) Human cytomegalovirus Fcgamma binding proteins gp34 and gp68 antagonize Fcgamma receptors I, II and III. *PLoS Pathog* 10(5):e1004131.
51. Stanton RJ, *et al.* (2010) Reconstruction of the complete human cytomegalovirus genome in a BAC reveals RL13 to be a potent inhibitor of replication. *J Clin Invest* 120(9):3191-3208.
52. Murrell I, *et al.* (2016) Genetic Stability of Bacterial Artificial Chromosome-Derived Human Cytomegalovirus during Culture In Vitro. *J Virol* 90(8):3929-3943.
53. Stanton RJ, McSharry BP, Armstrong M, Tomasec P, & Wilkinson GW (2008) Re-engineering adenovirus vector systems to enable high-throughput analyses of gene function. *Biotechniques* 45(6):659-662, 664-658.
54. Seirafian S (2012) An analysis of human cytomegalovirus gene usage. *PhD thesis, Cardiff University* (orca.cf.ac.uk/46644/).
55. Aoki J, Koike S, Ise I, Sato-Yoshida Y, & Nomoto A (1994) Amino acid residues on human poliovirus receptor involved in interaction with poliovirus. *J Biol Chem* 269(11):8431-8438.
56. Tomasec P, *et al.* (2005) Downregulation of natural killer cell-activating ligand CD155 by human cytomegalovirus UL141. *Nat Immunol* 6(2):181-188.
57. Prod'homme V, *et al.* (2007) The human cytomegalovirus MHC class I homolog UL18 inhibits LIR-1+ but activates LIR-1- NK cells. *J Immunol* 178(7):4473-4481.
58. Wang EC, *et al.* (2002) UL40-mediated NK evasion during productive infection with human cytomegalovirus. *Proc Natl Acad Sci U S A* 99(11):7570-7575.
59. Cox J & Mann M (2008) MaxQuant enables high peptide identification rates, individualized p.p.b.-range mass accuracies and proteome-wide protein quantification. *Nat Biotechnol* 26(12):1367-1372.

Figure Legends

Figure 1: HCMV infection down-regulates cell surface CD58

Human fibroblast (HF-TERT) cells infected with **(A)** HCMV strain Merlin or **(B)** strains Merlin or AD169 (MOI=5) or **(A, B)** mock-infected, and analyzed at the indicated time points post-infection by flow cytometry for cell surface expression of CD58 and MHC class-I. cIgG = isotype control IgG.

Figure 2: CD58 cell surface down-regulation is mediated by UL148

(A) Human fibroblast (HF-TERT) cells infected with a library of HCMV strain Merlin deletion mutants, (MOI=5, 72h post infection) and **(B)** human fibroblast (HF-CAR) cells infected with a library of adenovirus vectors encoding HCMV strain Merlin UL/b' genes, (MOI=5, 48h post-infection) as indicated were analyzed by flow cytometry for cell surface expression of CD58 and MHC class-I. MHC class-I down-regulation, which is a standard marker of HCMV infection, was used for quality control. Median fluorescence intensity (MFI) values relative to control cells (set to 1) are shown. **(C, D)** Representative plots from panels **(A)** and **(B)**, respectively. **(E)** Scatterplot of cell surface proteins modulated by UL148 analyzed by plasma membrane profiling. The complete data spreadsheet is shown in SI3. Proteins that contained Ig-/ MHC/ Cadherin/ C-type lectin/ TNF InterPro functional domains were included in the scatterplot. Significance B was used to estimate p values (59). The complete data spreadsheet is shown in Dataset S1.

Figure 3: UL148 retains immature CD58 intracellularly and interacts with CD58

Human fibroblast (HF-TERT) cells were infected (MOI=5) with HCMV strain Merlin (HCMV) or a UL148 deletion mutant (ΔUL148) and lysates were analyzed by immunoblotting **(A)** at the indicated time points post-infection or **(B)** 72h post-infection. EndoH or PNGaseF glycosidases were used as indicated. CD155, which is known to be retained in the ER by HCMV UL141 and actin were used as controls. **(C)** HF-TERT cells were infected with HCMV strain Merlin (HCMV) or HCMV recombinants expressing V5-tagged UL148 (HCMVUL148.V5) or UL141 (HCMVUL141.V5) and whole cell lysates (WCL) were analyzed by immunoblotting or co-immunoprecipitation (V5-IP). The known interaction between CD155 and UL141 served as a control.

Figure 4: UL148 modulates CTL function against HCMV-infected cells through CD58

(A) Human dermal fibroblast (D007) cells were infected with HCMV strain Merlin (HCMV) or an UL148 deletion mutant (ΔUL148) (MOI=10, 72h). Cells were pulsed with VLE or NLV peptide at 1 μg/ml and used in standard CD107 degranulation assay as targets for VLE-

or NLV-specific T-cell lines generated from donor D007. Means + SEM of quadruplicate samples are shown. **(B)** Expression of CD58 and MHC class-I on D007 cells. **(C)** Summary of HCMV vs HCMVΔUL148 data from 5 separate experiments standardizing values to the mock-infected control at the peptide concentrations indicated. One-way ANOVA with Tukey (for >5 means) multiple comparison post-hoc tests showed significance differences between HCMV and HCMVΔUL148 at *** p<0.001. **(D)** Effect of anti-CD58 mAb or an isotype control added at the start of assays to a concentration of 10μg/ml at the indicated peptide concentrations. Means + SEM of quadruplicate samples are shown. **(E)** Summary data of 3 different blocking experiments following standardization to isotype control values. **(F)** Further blocking assay on uninfected fibroblasts at lower concentrations of peptide pulsing. One-way ANOVA with Tukey (for>5 means) multiple comparison post-hoc tests showed significance differences at ** p<0.01 and *** p<0.001. **(G)** Degranulation of $CD3^+CD8^+$ T-cells in PBMC of 9 HCMV-seropositive donors challenged with autologous fibroblasts infected with HCMV strain Merlin or HCMVΔUL148 in the absence of peptide (MOI=10, 72h). Points are means of triplicate samples. Paired t-Test showed the p value indicated. # marks the 3 of 9 donors showing significant differences (p<0.05) when comparing responses between Merlin and HCMVΔUL148 using one-way ANOVA with Tukey multiple comparison post-hoc tests with %change from the Merlin response indicated in brackets.

Figure 5: Deletion of UL148 alters the response of NK cells

Fibroblasts were infected with HCMV strain Merlin (HCMV) or a UL148 deletion mutant (ΔUL148) (MOI=10, 72h). Cytotect or HCMV-negative IgG was added to a final concentration of 50 μg/ml. The cells were used to stimulate PBMCs from healthy donors stimulated overnight with 1000 IU/ml IFNα. $CD3^-CD56^+$ NK cell responses to allogeneic fibroblast (HF-TERT) cells from **(A)** a representative donor and **(B)** ten donors comparing responses with control HCMV-negative IgG and Cytotect. $CD3^-CD56^+$ NK cell responses to autologous dermal fibroblasts are shown in **(C)** with a summary of nine donors comparing responses with control HCMV-negative IgG and Cytotect. Allogeneic ADCC responses were further split into **(D)** $CD57^-$ and $CD57^+$ NK responses, and **(E)** $CD57^-$ $NKG2C^-$, $CD57^+NKG2C^+$ and $CD57^+NKG2C^-$ NK responses in 7 to 9 subjects. Data passed D'Agostino & Pearson omnibus normality testing. Points are mean of triplicate cultures. Paired t-Test showed the indicated significance p values. # marks donors showing significant differences (p<0.05) when comparing individual responses between Merlin and HCMVΔUL148 using one-way ANOVA with Tukey multiple comparison post-hoc tests. (2C-) indicates $NKG2C^-$ subjects, detected by flow cytometry.

Figure 1

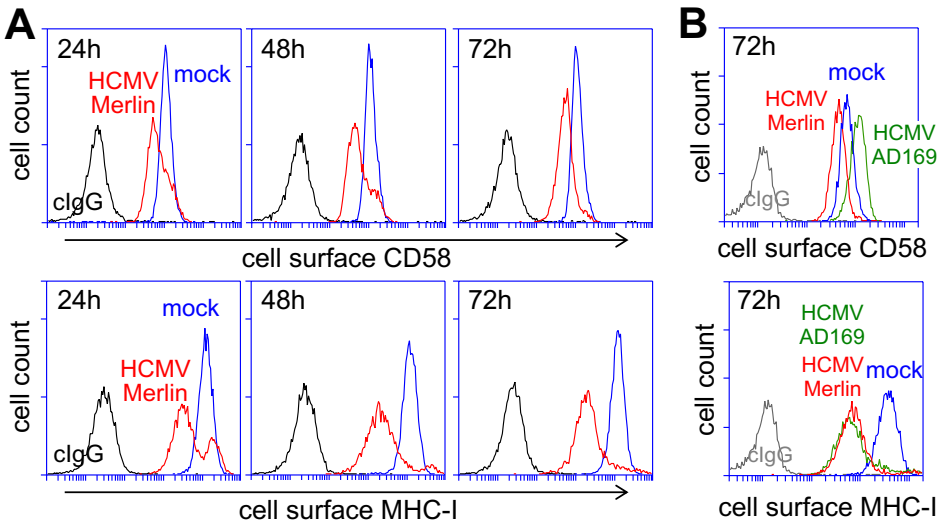
A
24h
48h
72h
HCMV
Merlin
mock
cIgG
cell count
cell surface CD58
24h
48h
72h
mock
HCMV
Merlin
cIgG
cell count
cell surface MHC-I
B
72h
mock
HCMV
Merlin
HCMV
AD169
cIgG
cell count
cell surface CD58
72h
HCMV
AD169
HCMV
Merlin
mock
cIgG
cell count
cell surface MHC-I

Figure 2

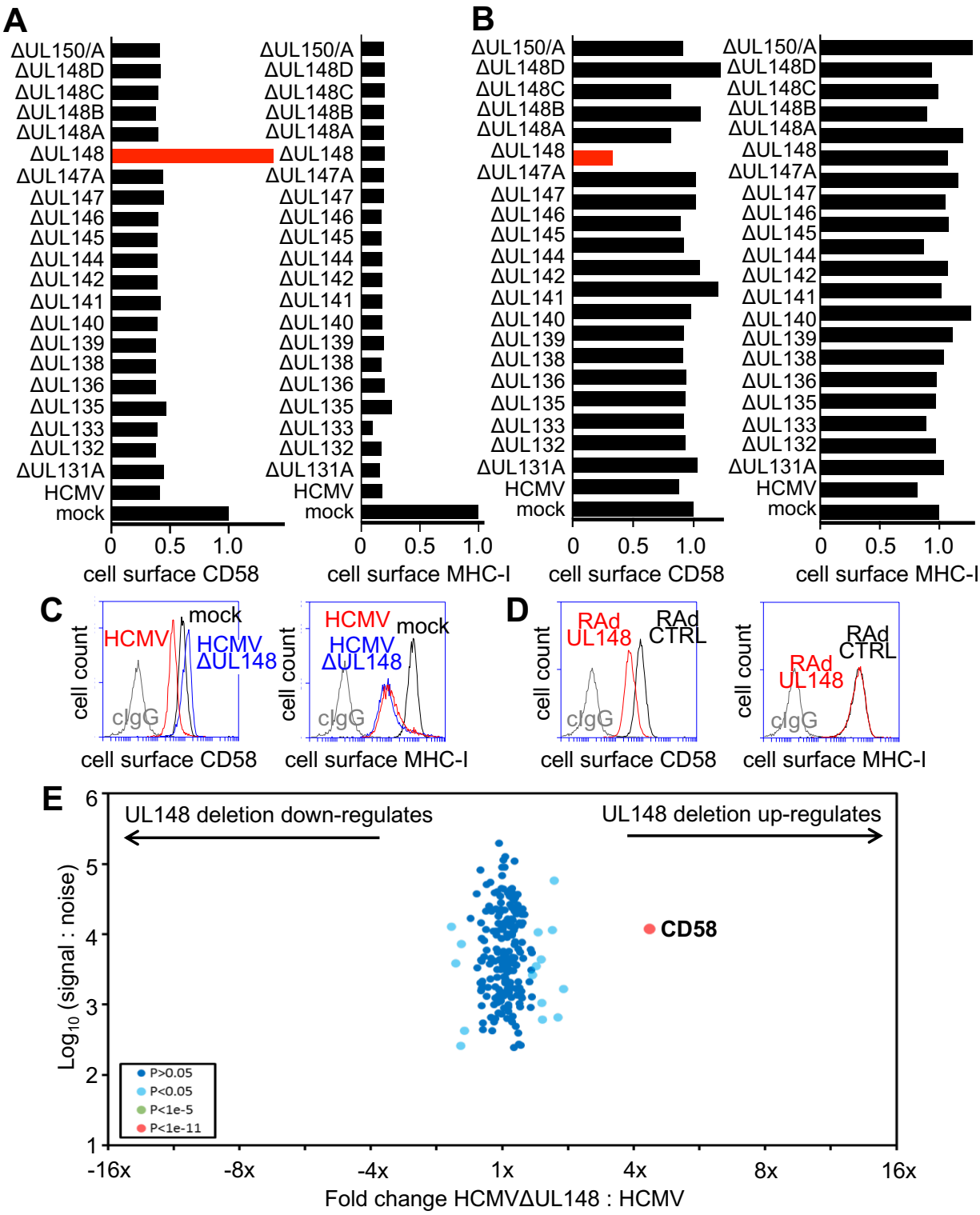
A
ΔUL150/A
ΔUL148D
ΔUL148C
ΔUL148B
ΔUL148A
ΔUL148
ΔUL147A
ΔUL147
ΔUL146
ΔUL145
ΔUL144
ΔUL142
ΔUL141
ΔUL140
ΔUL139
ΔUL138
ΔUL136
ΔUL135
ΔUL133
ΔUL132
ΔUL131A
HCMV
mock
0 0.5 1.0
cell surface CD58
cell surface MHC-I
B
C
cell count
HCMV
mock
HCMV ΔUL148
cIgG
D
RAd UL148
RAd CTRL
E
UL148 deletion down-regulates
UL148 deletion up-regulates
CD58
Log10 (signal : noise)
P>0.05
P<0.05
P<1e-5
P<1e-11
-16x -8x -4x 1x 4x 8x 16x
Fold change HCMVΔUL148 : HCMV

Figure 3

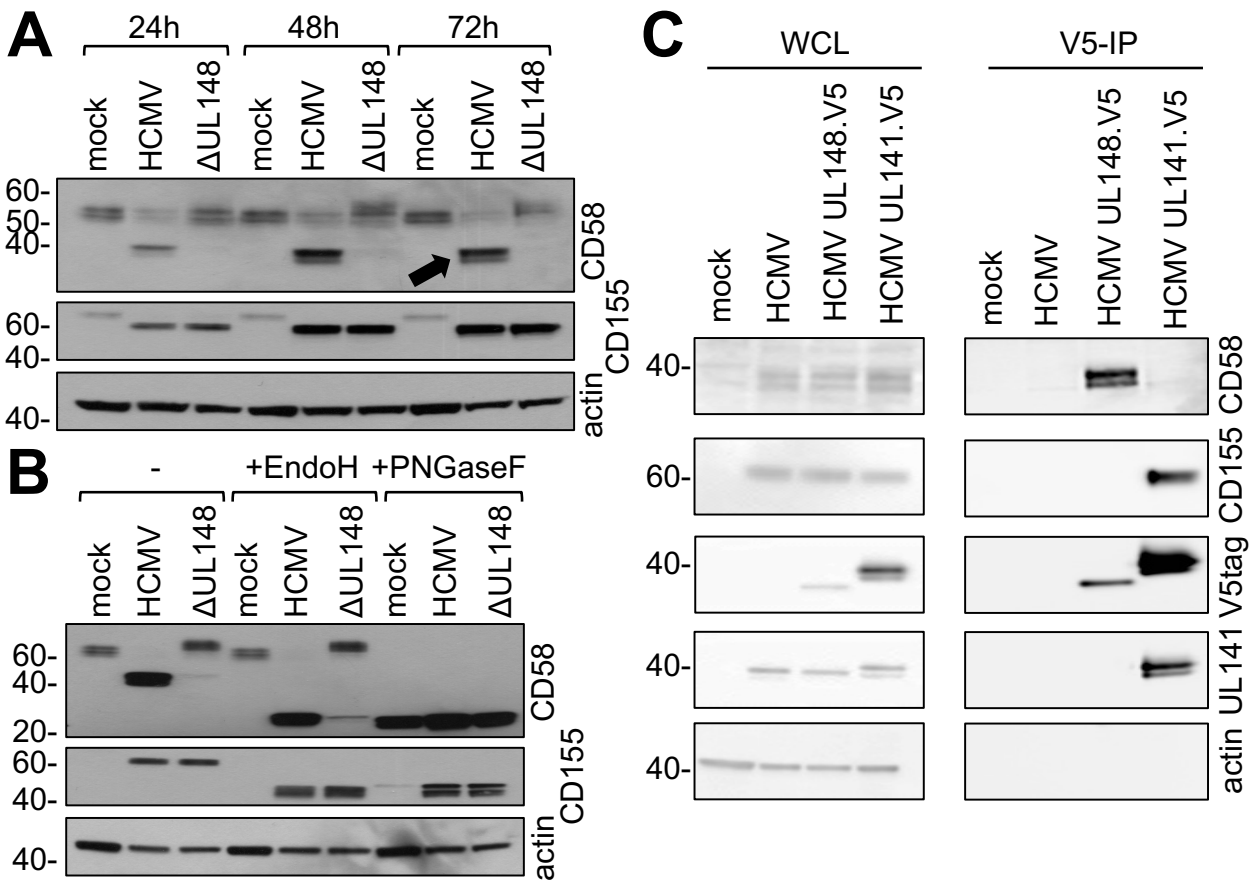
A
24h
48h
72h
mock
HCMV
ΔUL148
60-
50-
40-
CD58
CD155
actin
B
-
+EndoH
+PNGaseF
20-
C
WCL
V5-IP
HCMV UL148.V5
HCMV UL141.V5
V5tag
UL141

Figure 4

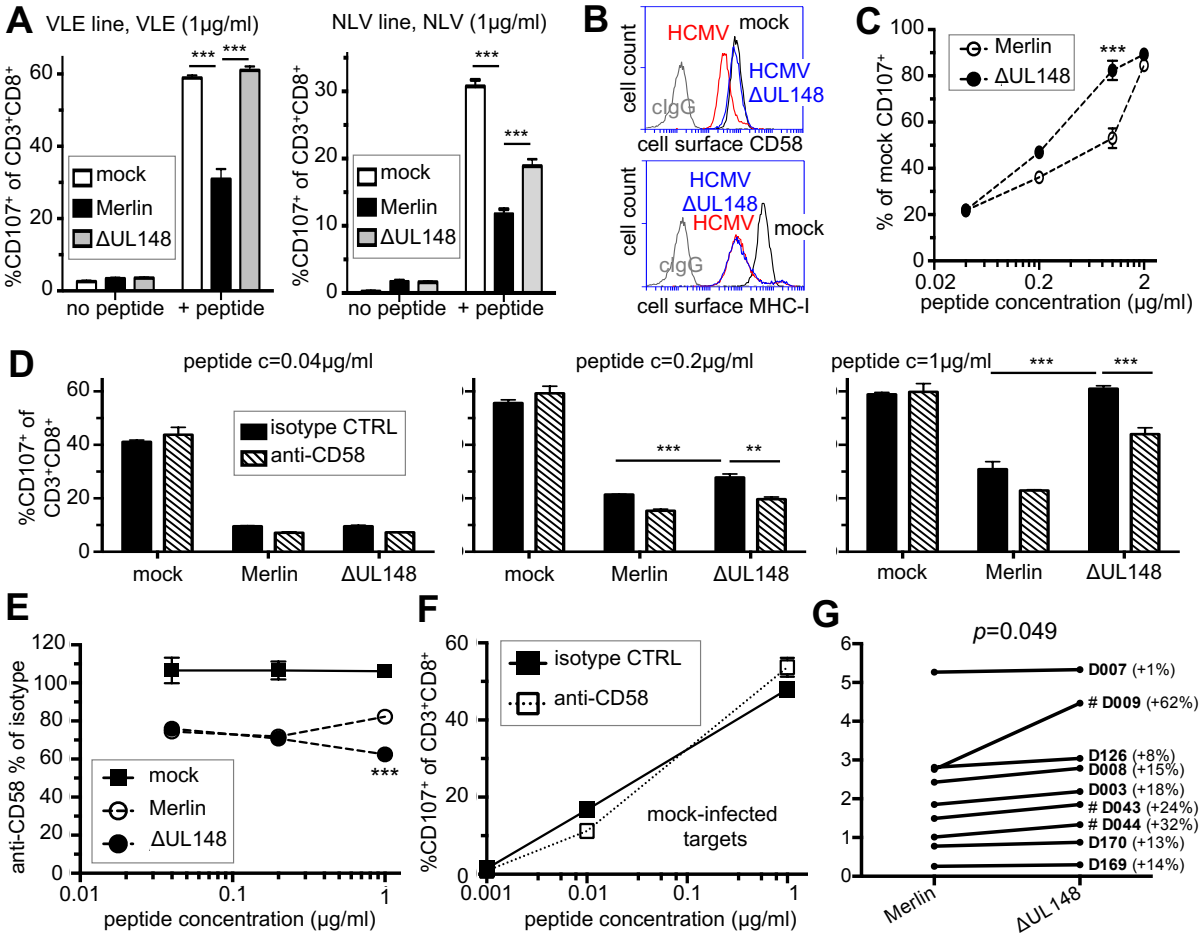
A
VLE line, VLE (1µg/ml)
NLV line, NLV (1µg/ml)
%CD107+ of CD3+CD8+
mock
Merlin
ΔUL148
no peptide
+ peptide
B
HCMV
mock
HCMV ΔUL148
cIgG
cell count
cell surface CD58
cell surface MHC-I
C
Merlin
ΔUL148
% of mock CD107+
peptide concentration (µg/ml)
D
peptide c=0.04µg/ml
peptide c=0.2µg/ml
peptide c=1µg/ml
isotype CTRL
anti-CD58
E
anti-CD58 % of isotype
F
mock-infected targets
G
p=0.049
D007 (+1%)
D009 (+62%)
D126 (+8%)
D008 (+15%)
D003 (+18%)
D043 (+24%)
D044 (+32%)
D170 (+13%)
D169 (+14%)

Figure 5

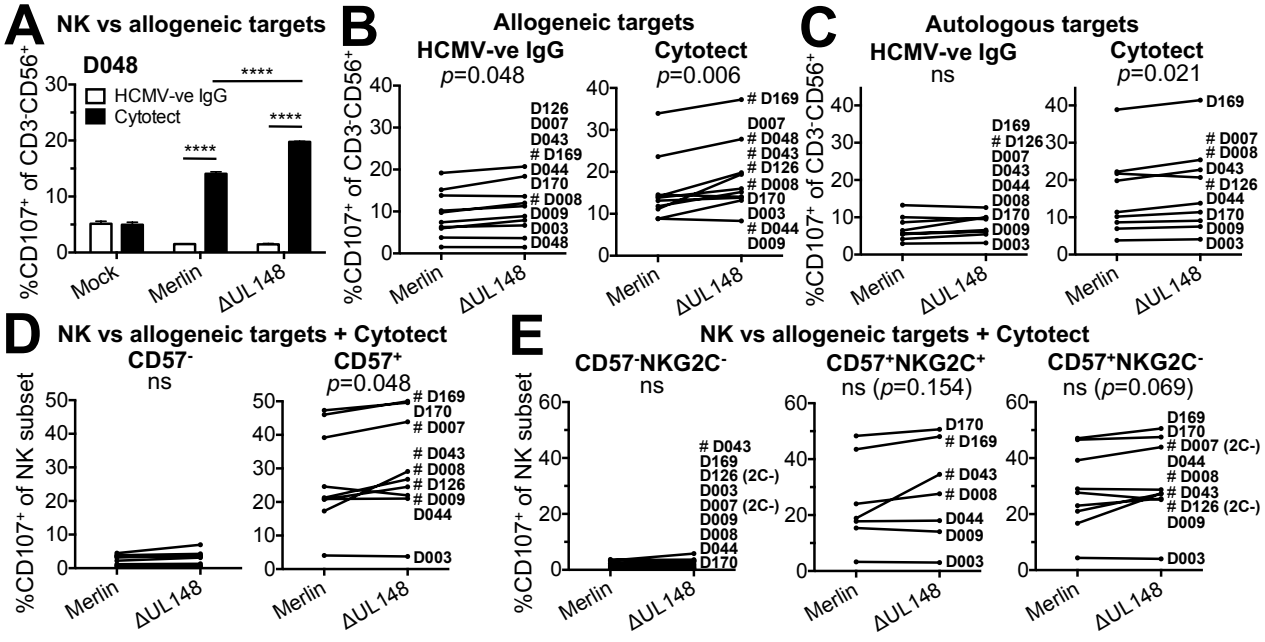
A
NK vs allogeneic targets
D048
HCMV-ve IgG
Cytotect
%CD107+ of CD3-CD56+
Mock
Merlin
ΔUL148
B
Allogeneic targets
HCMV-ve IgG
p=0.048
Cytotect
p=0.006
C
Autologous targets
HCMV-ve IgG
ns
Cytotect
p=0.021
D
NK vs allogeneic targets + Cytotect
CD57-
ns
CD57+
p=0.048
%CD107+ of NK subset
E
NK vs allogeneic targets + Cytotect
CD57-NKG2C-
ns
CD57+NKG2C+
ns (p=0.154)
CD57+NKG2C-
ns (p=0.069)

Supplemental Information Legends

Figure S1: Details of the library of HCMV recombinants containing single gene deletions

Recombinant HCMVs (RCMVs) were generated by recombineering of the strain Merlin bacterial artificial chromosome BAC1111/KM192298 (RL13^{-}, UL128^{-}) (Stanton RJ, *et al*. (2010). *J Clin Invest* 120: 3191-3208). Whole-genome consensus sequences of passage 1 of each RCMV were derived by using the Illumina platform as described previously (Fielding CA*, et al.* (2014). *PLoS Pathog* 10: e1004058), and were deposited in GenBank. Deleted regions are shown between slashes in lower case, with the initiation codon underlined, and did not always include the whole protein-coding region. Except for the differences noted, the viruses were genetically identical to that recovered from the parental BAC (RCMV1111/KM192298).

* middle G tract near right end of US is 1 bp shorter

** contains an 1190 bp *E. coli* insertion element IS150 plus a 3 bp duplication at the right end inserted into US11. This insertion was considered irrelevant to this study, but the recombinant was not banked for further use and the sequence was not deposited in GenBank.

Two further recombinants (not listed) were also constructed and their whole-genome sequences verified. To insert a V5 tag after UL148 (RCMV2084), a recombineering cassette comprising KanR/rpsL/lacZ was amplified and inserted into the 5' end of UL148 by using primers UL148 SacB Forward GCATTCTCGAGACGTGGCGACGTGGATTTCTTGCTATGTCCGCGAACGACGTGTGACGAGGACGTGGTTTCCGCAAGCCTCCTGTGACGGAAGATCACTT, UL148 Sac B Reverse TCAACACATTGCTGATTACAATGATGGCGGCGATATGGGCTCGCGTTTTGATAACCTACCTGGTGTCGCGGCGTCGGTAGCTGAGGTTCTTATGGCTCTT-3'. In a second round of recombineering, this cassette was removed and replaced by a V5 tag by using the complementary primers TGCTATGTCCGCGAACGACGTGTGACGAGGACGTGGTTTCCGCAAGCCTTTACGTAGAATCAAGACCTAGGAGCGGGTTAGGGATTGGCTTACCAGCGCT

And

GGCGATATGGGCTCGCGTTTTGATAACCTACCTGGTGTCGCGGCGTCGGAGCGCTGGTAAGCCAATCCCTAACCCGCTCCTAGGTCTTGATTCTACGTAA

(V5 tag and linker underlined). To insert a V5 tag after UL141 (RCMV2022), the KanR/rpsL/lacZ was amplified and inserted at the end of UL141 using primers

AGGGGACGACGAGGCGGTGAGGGCTATCGACGCCTACCGACTTACGATAGTTACC
CCGGTGTTAAAAAGATGAAGAGGCCTGTGACGGAAGATCACTTCG and
GCATATTTTAATCACACTATTCACATTTCACACACTGCATTTTTTAACATCTTATTTTT
TTATTTTATGCGTGTTCTCACTGAGGTTCTTATGGCTCTTG
(regions of homology to UL141 underlined). This cassette was then removed and replaced with a V5 tag, using primers
GACGCCTACCGACTTACGATAGTTACCCCGGTGTTAAAAAGATGAAGAGGGGCTCC
GGGGGGTCGGGTGGAAGTGGCGGTAAGCCAATCCCTAACCCGCT
And
ACACACTGCATTTTTTAACATCTTATTTTTTTATTTTATGCGTGTTCTCACGTAGAATC
AAGACCTAGGAGCGGGTTAGGGATTGGCTTACCGCCACTTC (complementary regions that overlapped to generate the V5 tag underlined).

Figure S2: Transcriptome profiles of HCMV strain Merlin (RCMV1111) and ΔUL148 (RCMV2035)

(A) Whole-cell RNA was isolated from human fibroblast (HF-TERT) cells infected with HCMV strain Merlin (RCMV1111) or a UL148 deletion mutant ΔUL148 (RCMV2035) at 72 h post-infection. Transcriptome profiles were derived from directional Illumina RNA-Seq data generated from polyadenylated RNA. The genome is shown in five sections, with the inverted repeats shaded grey. Protein-coding regions and non-coding RNAs are shown by color- and white-shaded arrows, respectively, with gene nomenclature below, and introns as narrow white bars connecting exons. The colours of protein-coding regions indicate conservation among alpha-, beta- and gammaherpesviruses (core genes) or between beta- and gammaherpesviruses (subcore genes), with certain noncore genes grouped into related families. The yellow windows depict transcription profiles for rightward (magenta) and leftward (cyan) transcripts. The extent of transcription is plotted as $\log_{10}$ of the number of reads per nucleotide (calculated by Bowtie2 assembly against the RCMV2035 sequence) per million viral reads, the overall number of reads for RCMV2035) being normalised to that for RCMV1111. The number of viral reads (76 nucleotides) in the RCMV1111 and RCMV2035 datasets was 11,857,464 (48% of the total) and 12,178,576 (52%), respectively. Among the regions containing zero reads (scored -2) is UL148 in RCMV2035 (boxed). Except for UL148, the transcriptome profile of RCMV2035 was very similar to that of RCMV1111. **(B)** Histogram showing the relative proportion (%) of normalized sequence read counts mapping to individual HCMV protein-coding regions and noncoding RNAs in RCMV2035 compared with RCMV1111. In this experiment, and excluding UL148, transcription levels of the protein-coding regions and non-coding RNAs

were 105±16% of those in RCMV1111, ranging from 57% (UL146) to 183% (the region common to IRS1 and TRS1). Only UL148 was differentially expressed >2-fold.

Figure S3: Identification of cellular proteins interacting with UL148 via SILAC-IP

SILAC-labelled HFFF-TERT cells were infected (MOI=5, 72h) with unmodified HCMV strain Merlin (light-labeled cells), HCMVUL141.V5 (medium-labeled cells) or HCMVUL148.V5 (heavy-labeled cells) followed by immunoprecipitation of mixed lysates with anti-V5. Enriched proteins were digested with trypsin then subjected to mass spectrometry. To identify proteins that specifically interact with HCMV UL148, the following filters were employed: UL148:wt ratio of >2 and UL148:UL141 ratio of >2. UL141 served as an irrelevant control and did not interact with UL148 (heavy : light ratio = 1.3). Significance A was used to estimate p-values, which were adjusted for multiple hypothesis testing using the method of Benjamini-Hochberg (59).

Figure S4: Effect of UL148 on cytokine production

Autologous skin fibroblasts were infected with Merlin (HCMV) or a UL148 deletion mutant (ΔUL148) (MOI =10, 72h) and then used as targets against a $CD8^+$ T-cell line or PBMCs. CD107a degranulation and intracellular cytokine staining for IFNγ and TNFα were measured after 6h using standard procedures (Becton Dickinson). **(A, B)** Two separate experiments on a $CD8^+$ T-cell line (D009-VTE) at a cognate peptide dose of 1 µg/ml. **(C)** PBMC data gating on $CD57^+CD3^-CD56^+$ NK cells with targets in the presence of Cytotect. MFI = median fluorescence intensity for positive cells. Mean + SEM of quadruplicates shown. Two-way ANOVA comparing all means showed significance at *p<0.05, **p<0.01, ***p<0.001.

Dataset S1: Mass spectrometric analysis comparing Merlin and MerlinΔUL148

Excel spreadsheet, no figure legend provided.

Supplemental Figure S1

GenBank Accession Number	RCMV Serial Number	Deletion
KM192298	RCMV1111	HCMV strain Merlin, parental BAC
KP973627*	RCMV1819*	**UL131A**; GAGCAACGAC/acctcggtca...acagccg**cat**/GTTGCAGACT
KP973628	RCMV1821	**UL132;** TCCCAGTCCC/gagtttccaa...gggccgg**cat**/TCTCGAGACG
KP973629	RCMV1823	**UL133;** TCCGATGTCG/gtgttggcgg...cgcaacc**cat**/TGCTACTGCG
KP973630	RCMV1825	**UL136;** AGCGACAGCC/gctgccgtag...tgactga**cat**/ACTCTCTTTC
KP973636	RCMV1847	**UL138;** AAGACGATGA/acccgcgcgg...gatcgtc**cat**/GGTGACCGTC
KP973637	RCMV1849	**UL139;** GCAGCAGCTG/cagactttac...tccacag**cat**/GTTCGTTACT
KP973638	RCMV1851	**UL140;** AAAAACCGAG/gtggtcgccc...cgggggt**cat**/GACAAGTCTG
KP973625	RCMV1812	**UL142;** GCCATCCTGA/ggatgttagt...caatccg**cat**/ATTTTAATCA
KP973639	RCMV1853	**UL144;** ATATGTGCGG/tatgattttg...gaggctt**cat**/GCCTCCTACC
KP973631	RCMV1835	**UL145;** GGAGCATCTC/aacaggcatg...cgccgta**cat**/CGAAGGCAAC
N.A. **	RCMV1837**	**UL146;** TGATGGGGCG/ataaacatac...ttaatcg**cat**/TATAATTTTA
KP973626	RCMV1814	**UL147;** CCAGCACTTC/ctgacgattg...ttagcaa**cat**/ATTGAAAACA
KP973640	RCMV1855	**UL147A;** ATAGTCTTGC/tcttcgcgaa...atagggaa**cat**/GATCACCAGC
KP973642	RCMV2035	**UL148;** CCGCAAGCCT/ctaccgacgc...agcgcaa**cat**/GCTGCGCGGG
KP973632	RCMV1839	**UL148A;** CGTCTCATCT/ttgccacagc...cggaact**cat**/GGCTATCGCC
KP973633*	RCMV1841*	**UL148B;** CTAAGGCCGT/gtcgccaacg...ccagcgc**cat**/CCCGTTCGCT
KP973634	RCMV1843	**UL148C;** CCGCGAGCAA/**atg**ttaactc...gaccttcgtg/CGTTGTCTCG
KP973635	RCMV1845	**UL148D;** GAGTCGCGGC/**atg**acggcgc...cagcagcagg/CACGCAACGG
KP973641	RCMV1857	**UL150/150A;** GTTTGCGGTC/tgcggtaagt...gtgtgag**cat**/AGCTGTATGC

Supplemental Figure S2

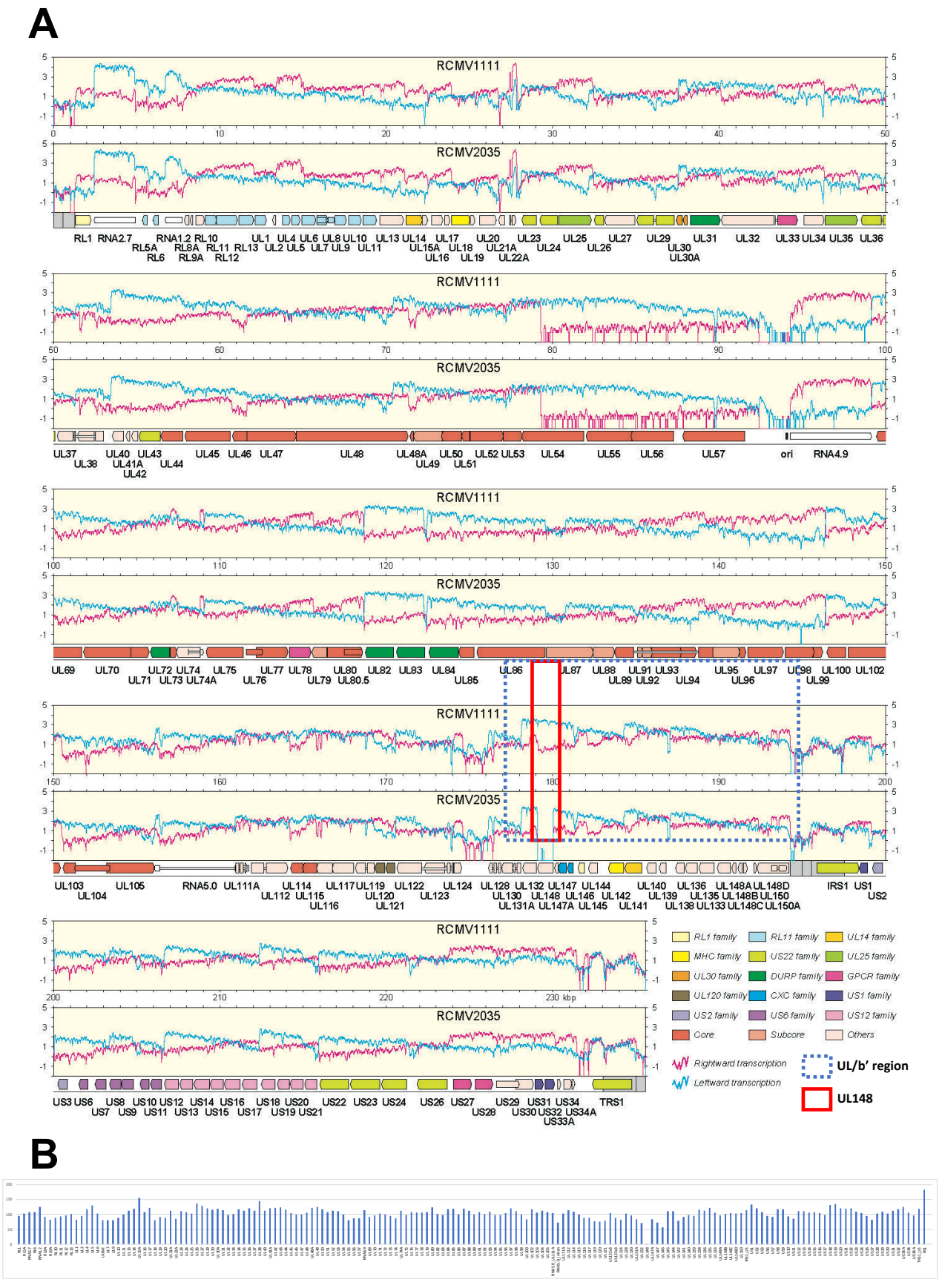

Supplemental Figure S3

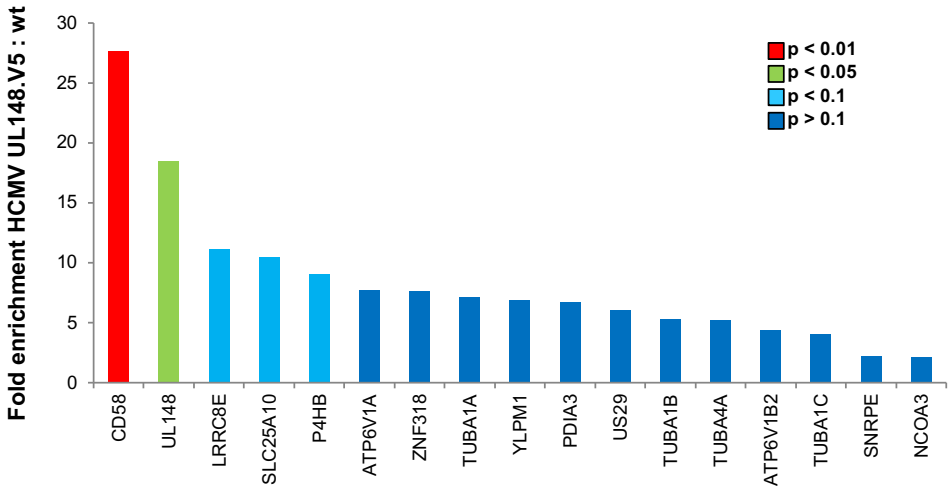

Supplemental Figure S4